Visual Abstract

Multiple linear regression parameters for determining fatigue-based entropy characterisation of magnesium alloy

M.A. Fauthan, S. Abdullah
Universiti Kebangsaan Malaysia, Malaysia
akashah948@gmail.com, shahrum@ukm.edu.my

M.F. Abdullah
Universiti Pertahanan Nasional, Malaysia
m.faizal@upnm.edu.my

I.F. Mohamed
Universiti Kebangsaan Malaysia, Malaysia
intanfadhlina@ukm.edu.my

ABSTRACT. This paper presents the development of the multiple linear regression approach based on the stress ratio and applied load that was assessed using entropy generation. The energy dissipation is associated with material degradation to determine the fatigue life with consideration to the irreversible thermodynamic framework. This relationship was developed by predicting a complete entropy generation using a statistical approach, where a constant amplitude loading was applied to evaluate the fatigue life. By conducting compact tension tests, different stress ratios were applied to the specimen. During the tests, the temperature change was observed. The lowest entropy generation was 2.536 MJm^{-3} K^{-1} when 3,000N load with a stress ratio of 0.7 was applied to the specimen. The assumptions of the models were considered through graphical residual analysis. As a result, the predicted regression model based on the applied load and stress ratio was found to agree with the results of the experiment, with only 9.3% from the actual experiment. Therefore, the entropy generation can be predicted to access the dissipated energy as an irreversible degradation of a metallic material, subjected to cyclic elastic-plastic loading. Thermodynamic entropy is shown to play an important role in the fatigue process to trace the fatigue life.

KEYWORDS. Entropy; Fatigue Crack Growth; Magnesium alloy; Multiple Linear Regression; Stress ratio.

OPEN ACCESS

Citation: Fauthan, M. A., Abdullah, S., Abdullah, M. F., Mohamed, I. F., Multiple linear regression parameters for determining fatigue-based entropy characterisation of magnesium alloy, Frattura ed Integrità Strutturale, 62 (2022) 289-303.

Received: 31.03.2022
Accepted: 29.06.2022
Online first: 31.08.2022
Published: 01.10.2022

INTRODUCTION

The growing ecological effect of transport emissions, limited resources, and the restraint to conserve energy has resulted in a comprehensive research study that focused on establishing innovative magnesium alloys for light-weight automobile structural applications. To ensure the safe and reliable applications of Mg alloys, the fatigue deformation resistance of Mg alloys has to be studied. Since magnesium alloy has a very low weight for its capability and workability, industries make a high usage of magnesium alloys in many mechanical functions [1]. If the parts are exposed to load in cyclic conditions, the determination of fatigue properties becomes crucial. As a progressive reduction of the material strength process, fatigue will occur due to cyclic loading or cyclic contortion. Fatigue failure can happen suddenly with no obvious caution and typically catastrophically [2]. It starts with the development of microcracks that continue to grow with duplicated applications of the load [3]. This concurrently decreases the product's recurring strength until becomes so low that the structure's failure is impeded [4]. Fatigue problems are often the main problem of total performance, which thus calls for an investigation of magnesium alloys' fatigue characteristics [5].

At the beginning of the research, common fatigue analysis methods include stress-life curves for high-cycle fatigue (HCF) and strain-life curves for low-cycle fatigue (LCF). Existing approaches sometimes give inconsistent results, and failure measures usually depend on the environment set up. Recent entropy-based fatigue studies have shown high accuracy, establishing thermodynamic energies and entropies as measures of system damage, degradation and failure.

The fatigue procedure is typically accompanied by energy change, which establishes a thermodynamic structure to study its depiction. As the irreversible process occurs, the energy dissipates, which shows that the concept of entropy is a suitable tool to review the fatigue process [6]. In this case, entropy generation is an early detection mode that allows the researcher to develop the approach from the surface temperature evolution. The use of the energy theory to study fatigue is another approach to determining fatigue life. Most works were conducted based on the total strain energy density, which has been widely used to evaluate material failure. Over the past several decades, thermodynamic measurements have also been widely used with fatigue tests as non-destructive testing (NDT) method, mainly to determine fatigue properties.

Furthermore, some researchers [7] have examined the theoretical structure and comparable testing methods to analyse dissipated heat energy at the crack tips. The elastic-plastic fracture parameter shows the average heat energy in a cycle [8]. It was found that the fatigue damage can be depicted as an index for energy dissipation in a system volume cycle [9]. The fatigue process in mechanical processes uses the concept of the thermodynamics structure [10], which is not unanticipated as fatigue deterioration is an irreversible process that slowly ages a system until failure by fracture [11]. The second law of thermodynamics is related to fatigue, where entropy is generated during the disorder [12]. Typically, fatigue is a complicated procedure that is impacted by different aspects. Problems in fatigue research study occur due to the presence of many internal and external aspects such as the properties of the material as well as the load and geometry which affect fatigue behaviour [13]. After that, various approaches and theories have been used to design and study fatigue procedures, for instance, the variety of cyclic loading before fracture [14], dissipated energy [15], and deterioration in structural applications [16]. Current research studies in infrared thermography for non-destructive examination of damage have offered brand-new research studies for the research findings the study of crack propagation for specimens subjected to cyclic loading [17]. In a traditional test, numerous unidentified input specifications are needed. Furthermore, this relationship can be described through the introduction of multiple linear regression (MLR) to predict a variable's value based on the importance of two or more other variables.

Earlier research studies have shown that the evolution of temperature throughout fatigue failure can be utilised as a primary forecast of fatigue life [18]. To examine fatigue failure based on entropy generation, the temperature level difference throughout the fatigue system is essential [19]. If the total generation of entropy can be approached through regression, then fatigue life can be predicted. Hence, this paper aims to describe the MLR relationship to predict the total entropy generation of magnesium alloy, AZ31B.

LITERATURE BACKGROUND

The thermodynamic approach to assessing materials' fatigue behaviour requires the definition of a system that obeys thermodynamics laws. For practical purposes, it is considered that the material subjected to the analysis is a closed system since there is no mass inter-change with the environment, even though there is heat transfer through the boundaries.

The dissipative process during the energy transformation can be assumed as fatigue damage. Typically, it is presumed that, for a volume of product V going through cyclic loadings, the power W used up in one cycle is either dissipated as heat (Q)

or taken in to elicit variation of the internal energy (U) [20]. According to the first law of thermodynamics, the equation is expressed by:

$$W = Q + U \tag{1}$$

The advantage of utilising thermodynamic forces and flows is that the entropy production σ can be explained in terms of experimentally quantifiable amounts. For this reason, during the dissipative process, high-quality energy degrades to low-grade energy, which is a procedure called entropy generation [21].

ENTROPY GENERATION METHOD

In fatigue, the dissipative process $p = p(\zeta)$ depends on a time-dependent phenomenological variable ζ. When defined in general terms, the change in system's entropy, dS through a form of modification is connected to δQ by:

$$dS = \delta Q / T \tag{2}$$

where T is the temperature.
entropy production rate depends on dissipative process p, and its rate is $\sigma = ds/dt$

$$\sigma = \frac{d_i s}{dt} = \left(\frac{\partial_i s}{\partial p} \frac{\partial p}{\partial \zeta} \right) \frac{\partial \zeta}{\partial t} = XJ \tag{3}$$

where is $X = \frac{\partial_i s}{\partial p} \frac{\partial p}{\partial \zeta}$ the thermodynamics forces and $J = \frac{\partial \zeta}{\partial t}$ is the thermodynamics flows.
In this research, the dissipative process is the plastic strain involving fatigue [23]. The measure of system degradation, w. So, let D is the rate of degradation $D = dw/dt$:

$$D = \frac{dw}{dt} = \left(\frac{\partial w}{\partial p} \frac{\partial p}{\partial \zeta} \right) \frac{\partial \zeta}{\partial t} = YJ \tag{4}$$

From above equation, the degradation of the system varies in the same manner between dissipative process p and the entropy generation. The combined parameter in Eqns. (3) and (4) is the thermodynamic flow, J, a degradation coefficient can be expressed as:

$$B = \frac{Y}{X} = \frac{(\partial w / \partial p)(\partial p / \partial \zeta)}{(\partial_i s / \partial p)(\partial p / \partial \zeta)} = \left| \frac{\partial w}{\partial_i s} \right| \tag{5}$$

From Eqn. (4) and Eqn. (5), the degradation can be defined as:

$$D = \frac{da}{dt} = YJ = BXJ = B \frac{f}{T} \frac{dW_p}{dN} \tag{6}$$

Some researchers [25] have mentioned in their research that :

$$\frac{dW_p}{dN} = At \frac{(\Delta K)^4}{\mu \sigma_y^2} \tag{7}$$

Therefore,

$$\frac{da}{dN}=\frac{da}{fdt}=B\frac{At}{T}\frac{(\Delta K)^4}{\mu\sigma_y^2} \tag{8}$$

The following equation assumes the relationship between plastic deformation and the thermal dissipation in the second law of thermodynamics in solids with internal friction [26]:

$$\dot{\gamma}=w_p/T-J_q\cdot grad\,T/T^2 \tag{9}$$

In this instance $\dot{\gamma}$ signifies the rate at which entropy is manufactured ($\dot{\gamma}\geq 0$), J_q is the heat flux, T the temperature of the surface, and w_p is the recurring plastic energy mass per unit which comes from the calculation from Morrow's estimate [27].

$$w_p=AN_f^{\alpha} \tag{10}$$

constants A and a are from the material value, which can be found using this equation:

$$A=2^{2+b+c}\varepsilon_f'\sigma_f'\left(\frac{c-b}{c+b}\right)\left(N_f\right)^{b+c} \tag{11}$$

where ε_f' and σ_f' are cyclic ductility and fatigue strength coefficient, respectively. Then, the terms b and c are the fatigue strength exponent and the fatigue ductility exponent, respectively.

Multiple Linear Regression (MLR)

MLR was chosen to develop a relationship between entropy and the applied load as well as stress ratio to ensure the linear relation between dependent and independent variables. MLR is able to immediately predict the dependent variable by matching the observational data and thus eliminating the need for repeated research with commercial software. The general multiple regression model was defined to be:

$$f\left(x_i\right)=\alpha+\beta_1x_{i1}+\beta_2x_{i2}+\ldots.+\beta_nx_{in}+\varepsilon_i \tag{12}$$

MLR attempts to model the relationship between two or more explanatory variables and a response variable by fitting a linear equation to observed data. Every value of the independent variable is associated with a value of the dependent variable. From the Eqn. (12), $f\left(x_i\right)$ is the dependent variable (entropy of the material) and x_i is the *ith* independent variable. There are two independent variables in this study: (1) load applied and (2) stress ratio. ε_i represents the intercept, which is a constant, β_1 represents the slope of the linear relationship between the means of the dependent and independent variables, and e is the random error with a mean of 0. Additionally, this work aimed to provide a reliable solution to predict fatigue life.

Methodology

The methodology implemented in this study begins with the determination of fatigue crack growth and temperature evolution. In Fig. 1, the process flow of the study is shown. This paper starts from the material preparation until the development of MLR. After the material preparation, the fatigue crack growth test was conducted to determine the stress intensity factor using the Linear Elastic Fracture Mechanics (LEFM) principle. During the test, besides observing the

fatigue crack growth rate, the evolution of the surface temperature was also monitored. The collected data were used for further investigation on entropy generation. All the data needed to be validated before proceeding with the development of MLR.

The approach applied in this study begins by determining the fatigue crack development and the evolution of temperature. The study made use of the commercial AZ31B magnesium alloy. AZ31B is a wrought magnesium alloy with both notable room-temperature ductility and strength.

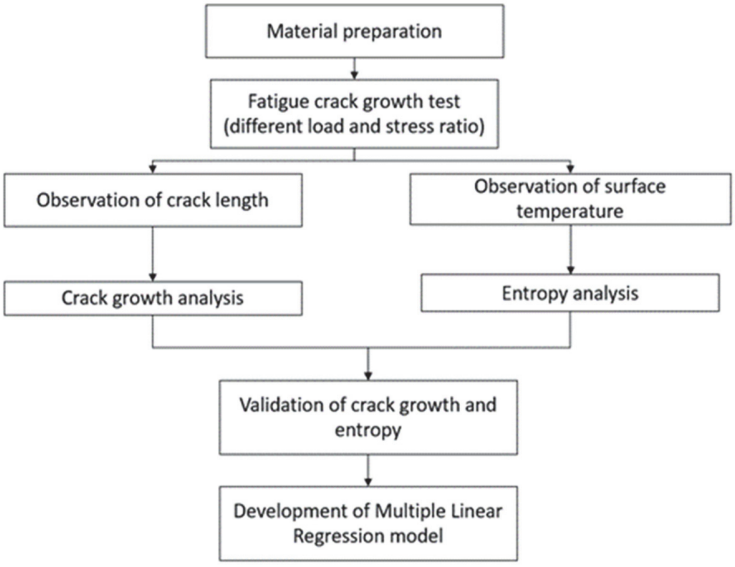

Figure 1: Process flow of crack growth and entropy generation

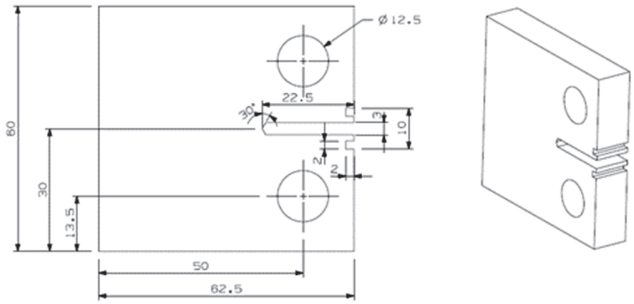

Figure 2: Geometry of the specimen with dimension in mm according to ASTM E647

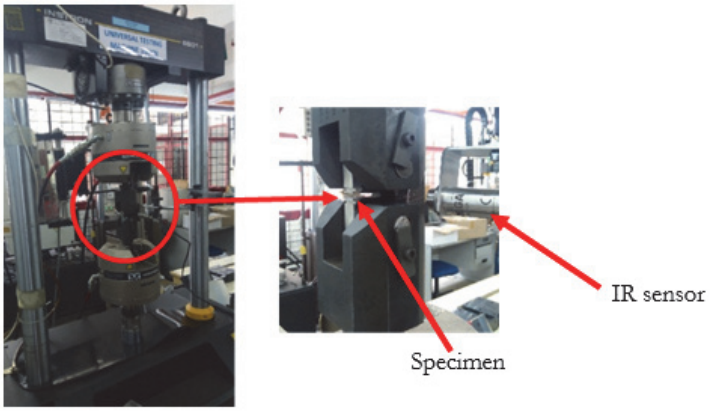

Figure 3: The setup of the IR sensor and the specimen

The AZ31B's mechanical properties are listed in Tab. 1. The thickness of the specimen is 10 mm.

Properties	
Young's modulus (GPa)	44.8
Poisson's ratio	0.3
Yield Strength (MPa)	244
UTS (MPa)	298

Table 1: Material properties of AZ31B [1]

The specimens of compact tension (*CT*) were prepared following the recommendation of the ASTM E647 standard document as illustrated in Fig. 2 to study the fatigue crack growth (FCG). The CNC milling machine and electrical discharge wire-cutting device were used to cut the sample to the required dimensions. The need to prepare a good quality sample is very important, which can be achieved by polishing and cleaning the sample using sandpaper with 600, 9000 and 1200 grids. Therefore, no oxides and grease on the specimen's surface are present to obtain accurate results during the thermos-effect measurement. Furthermore, the exclusion of stress concentration on the surface could prolong the beginning of the fatigue crack.

A uniaxial servo-hydraulic at a load capacity of 100kN was used to perform all the FCG experiments as in Fig. 3. The temperature of the surface material was monitored and recorded using the non-contact infrared sensor. The usage of an infrared sensor is to enable the measurement of small fluctuation of temperature due to elastic deformation during the test. Common equipment such as the thermocouple is not suitable for this set of tests.

The specimen used a constant amplitude sinusoidal loading with a different load (2,600 N, 2,800 N and 3,000N) and different load ratios (R = 0.1, 0.4 and 0.7) [24] with constant frequency of 10 Hz. According to previous work, to perform the LEFM method, the stress applied should not exceed 0.8σ of UTS. Considering the suitability of ΔK, the different load must be calculated using:

$$\Delta K = \frac{\Delta P}{B\sqrt{W}} \frac{2+\alpha}{(1-\alpha)^{3/2}} F_p \tag{13}$$

and

$$F_p = (0.886 + 4.64\alpha - 14.72\alpha^3 - 5.6\alpha^4) \tag{14}$$

B and W are the thickness of the specimen, F_p is the geometry factor and α is W/P where W/P should not exceed 0.2 as mentioned in the E647 standard document.

During the test, the specimen's temperature trend was detected with the infrared sensor which was set up with a 50 mm gap between the sensor and specimen according to the specification of the setting device.

RESULTS AND DISCUSSION

Fatigue crack growth

The crack caused by fatigue can be monitored from the experiment. From the beginning of the process, the crack initiation of the specimen was shown. At the loading of 2,600N, the crack began after 4,343 cycles, while for the 2,800N load, cracking began after 3,739 cycles. During the loading of 3,000N, the specimen recorded the lowest cycle at 2,288 compared to the others. The increment of the amplitude loading led to shorter fatigue life at 2.87 x 10^4, 2.70 x 10^4, and 2.55 x 10^4 cycles, respectively. The test also explains that if a different load of 2,600N, 2,800N, and 3,000N was applied, the curve varies from each other since the load of 2,600N with 0.1 stress ratio has the longest fatigue life. The

difference does not mean that the specimen has different material properties but that it needs to be analysed using the log-log curve.

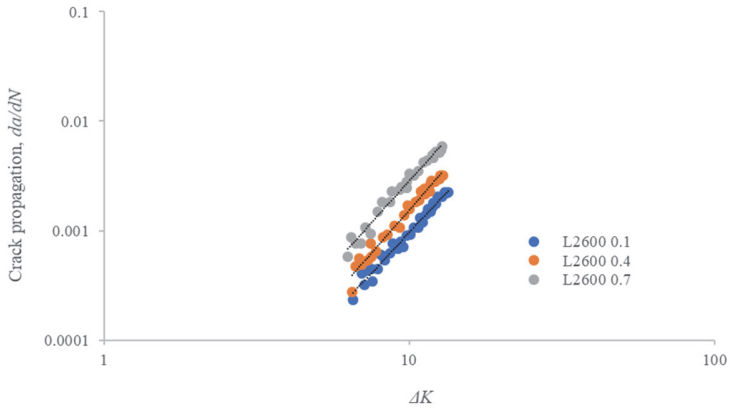

Figure 4: Fatigue crack growth curve for the AZ31B magnesium alloy for stress ratio 0.1, 0.4, 0.7 after 2,600N was applied.

Next, the correlation between calculated ΔK and crack growth is explored. The data attained from the experiment showed three different results even though the setup of the experiment was the same. However, the scattered band of fatigue crack growth rate was estimated to be the same in the log-log relationship. Fig. 4 depicts the confirmation of the linear relationship between da/dN and ΔK values in the double log scale. The constant m was calculated to be 3.6 for the stress ratio of 0.1, 0.4 and 0.7, while the C value was in the range of 1.0×10^{-7} to 3.0×10^{-10} (m/cycle)/ MPa.m$^{1/2}$.

Entropy generation

The evolution of the crack's temperature throughout the fatigue crack growth investigation for all loads applied and stress ratio is displayed in Fig. 5 (a). It shows that different loads with different stress ratios will give different results. Moreover, the results show that the value changes go through three different phases. However, the temperatures show the same trend. From Fig. 5 (b), at the beginning of the FCG test, which is in Stage 1, the sudden movement and the disruptions of the grains will cause a rise in the surface temperature, which concerns 10% of the material's lifecycle [21]. The phenomenon of intrusion and extrusion also occurs during this stage. After that, the temperature is more stable in Stage 2 as the volume of heat generated is the same as the heat released to the surrounding. However, at the end of the test, the temperature begins to increase in a short time due to the more extensive plastic deformation compared to the deformation that occurs in the second stage. There was a progressive increase in the rate of fatigue crack growth as they tend to become unstable in Stage 3 [11].

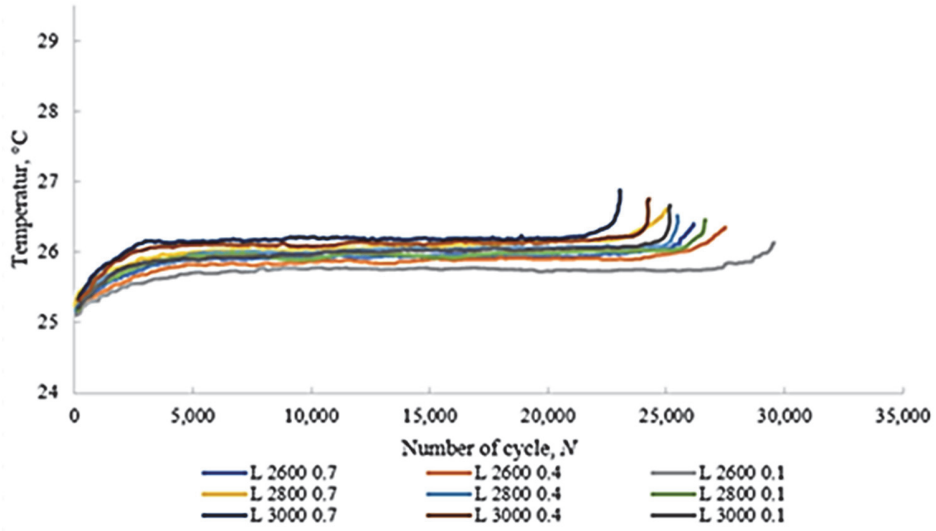

(a)

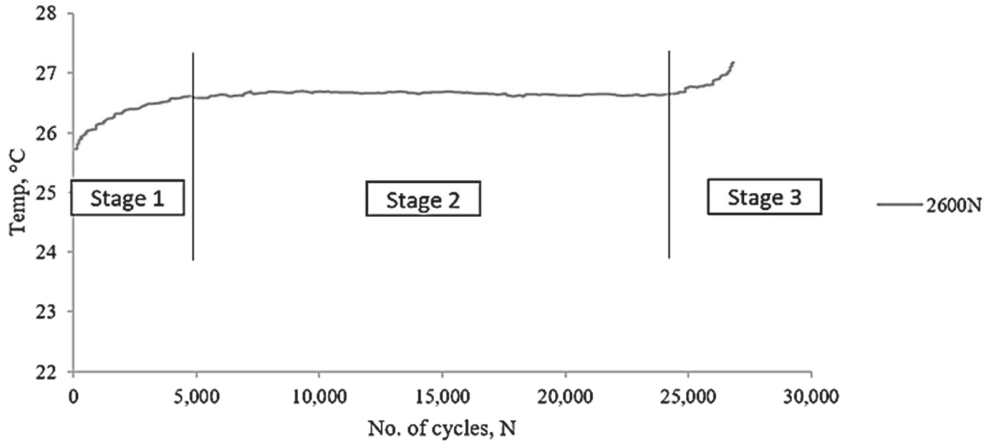

(b)

Figure 5: The temperature evolution measured during fatigue a crack growth tests: (a) three different load and stress ratio (b) under 2,600N for stress ratio 0.1.

From the experiment done, the development of the entropy generation for three various loads and three various stress ratios are different from each other. The temperature level utilised to examine the entropy generation remains in Kelvin. For the majority of the fatigue life, the entropy generation was almost consistent [28]. Entropy generation is $\dot{\gamma} = \frac{f \Delta w}{T}$ since the temperature evolutions are small.

For the purpose of comparison, the load of 2,600N is further investigated. Fig. 6 shows that the relation between the fatigue crack growth and the energy dissipation is in a linear function for the three different stress ratio tests. However, it is obvious that the gradients of the three graphs are of different values. The difference indicates that during the crack growth, there were different amounts of energy dissipation for the three different stress ratios. In other words, energy dissipation is dependent on the stress ratio value. From other research [29], the energy dissipation is independent with the dimension, load, and stress ratio to each material.

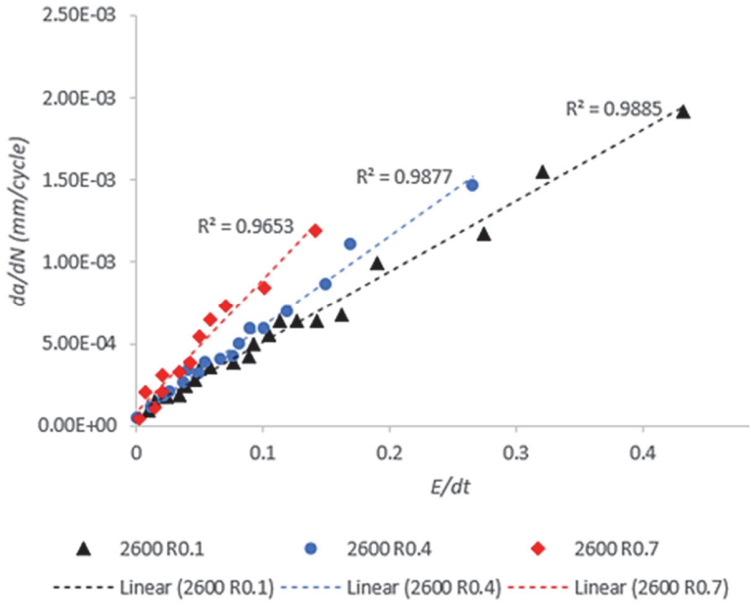

Figure 6: The energy dissipation during the fatigue crack growth for different stress ratio

However, the disparity on this matter can be explained in the relationship between ΔK and energy dissipation during the fatigue crack growth. The spread of the points in Fig. 7 is nearly at the same trend. The difference is at the end of the test,

where the lowest stress ratio, 0.1 showed the highest energy dissipated. This relationship shows that the energy dissipated is independent of the stress ratio.

As the crack growth increases, the total entropy was calculated until the specimen fractures utterly. The total entropy generation when a load of 2,600 N was applied was 3.424, 3.101 and 2.922 MJm^{-3} K^{-1} for stress ratios of 0.1, 0.4 and 0.7, respectively. According to Fig. 8, the total entropy generation decreased as a higher stress ratio was applied. This was due to the distribution of a higher energy per unit volume, which led to failure. It shows that with a higher entropy generation, the specimen should have a higher fatigue life. It shows that entropy generation with consideration to internal friction moved from a low value to a higher value as loads decreased due to the accumulation of internal friction.

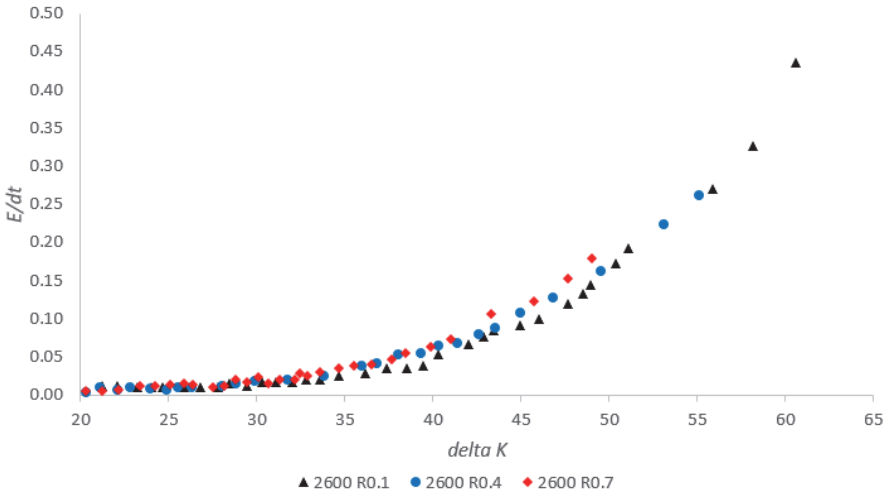

Figure 7: The relationship between energy dissipated rate and delta K in different stress ratio for 2600N

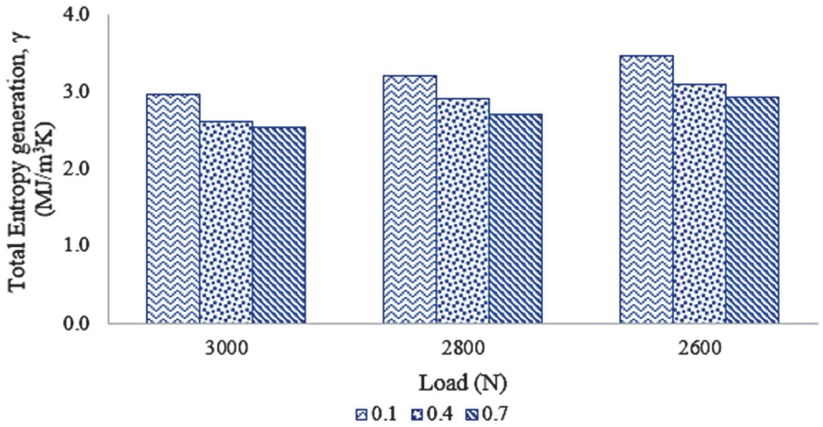

Figure 8: Total entropy generation with different loads and stress ratios.

Tab. 2 and Fig. 9 show the statistical analysis for the cycle count. It is evident that the distribution offered the best fit for the cycle count information according to the goodness of fit criteria. A probability distribution is an analytical function that explains all the values that are possible and the probabilities that a random variable can take within a bounded range. This range varies between the lowest and highest potential value, however, the possible value that is most likely to be outlined on the probability distribution depends on a variety of elements. The *p*-value of each load applied shows the value of 0.975, 0.973 and 0.940. The p-value is a probability that measures the evidence against the null hypothesis. Smaller p-values provide stronger evidence against the null hypothesis. To determine whether the data do not follow a normal distribution, compare the p-value to the significance level. Because the *p*-value was greater than the significance level of 0.05, the value is acceptable [30][31]. For example, a significance level of 0.05 indicates a 5% risk of concluding that a difference exists when there is no actual difference. The analytical chart reveals that the points fall within the self-confidence limitations, showing that the

straight line seems to have a relatively good fit for the data [32]. This suggests no proof that the value does not come from distribution for cycles count data of load used for 2,600N, 2,800N and 3,000N. It was evident that the distribution offered the best fit for the cycle count information according to the goodness of fit. Fig. 10 shows the entropy correlation between the predicted and experimental values. Correlation analysis is a method of statistical evaluation to study the strength of a relationship between two numerically measured and continuous variables. This method has been used by various researchers to calculate the accuracy of empirical data with the predicted fatigue life data. The plot shows that all points are fitted fit within the range of 1:2 and 2:1 correlation margin. As all of the points were scattered within the lines, the simulated and experimental fatigue lives were determined to be within the acceptable limit.

Load applied, N	Mean	St Dev	AD	P-value
2600	16467	7683	0.127	0.975
2800	16962	6270	0.128	0.973
3000	15446	6427	0.151	0.940

Table 2: The statistical results of cycles count data.

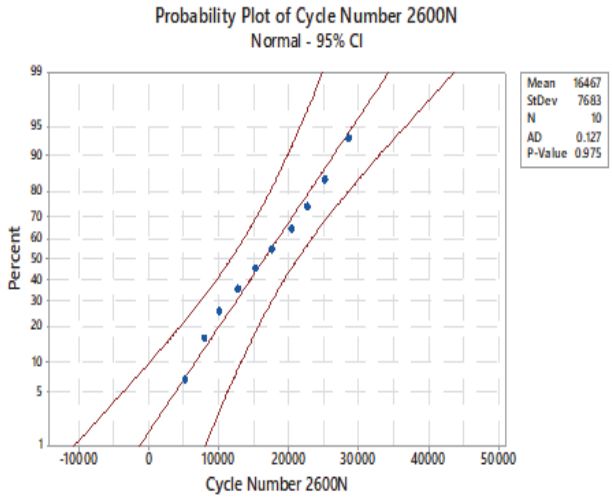

(a)

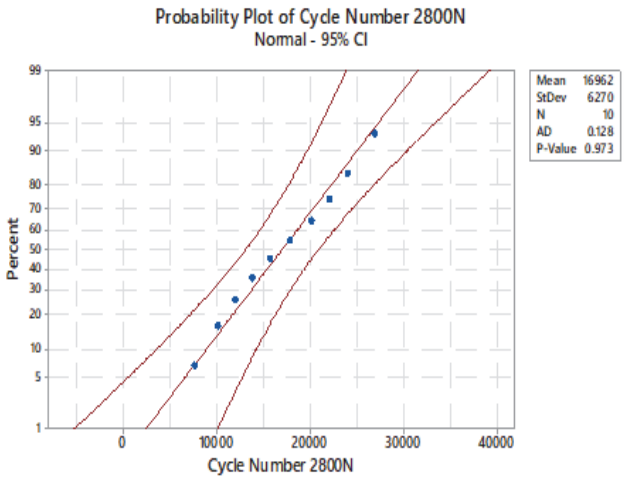

(b)

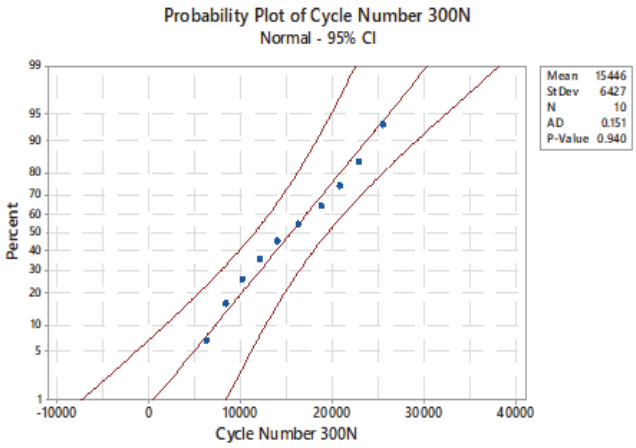

(c)

Figure 9: The probability distribution of fatigue crack growth at different load of (a) 2600N; (b) 2800N; (c) 3000N

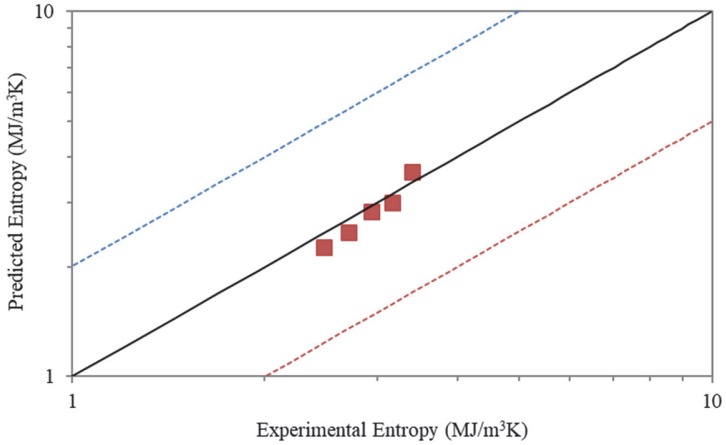

Figure 10: Relationship between predicted and experimental entropy

Multiple Linear Regression

To calculate the relationship between two or more independent variables and one reliant variable, MLR was utilised. The regression design can describe the indirect regression examination with just one explanatory variable by utilising a two-dimensional plot of the reliant variable as a function of the independent variable [33]. The regression has five key assumptions: 1) linear relationship, 2) multivariate normality, 3) no or little multicollinearity, 4) no autocorrelation, and 5) homoscedasticity. From the data set, the straight line can be obtained to represent the model of regression. Moreover, the R^2 value determines fit consistency. Nonetheless, there are many explanatory variables associated with MLR analysis and, as a result, the presumptions of linearity, homoscedasticity, and normality must be tested to confirm that the MLR-based entropy models obtained in this research can be generated with valid inferences. In statistics, the response surface methodology as in Fig. 11, explores the relationships between several explanatory variables and one or more response variables. Response surface plots such as contour and surface plots are useful for establishing desirable response values and operating conditions. In a contour plot, the response surface is viewed as a two-dimensional plane where all points that have the same response are connected to produce contour lines of constant responses. Overall, the response surface plot in Fig. 11 shows that the entropy varies inversely with the load applied and linearly with the stress ratio (independent variables), which validates the linearity of the MLR-based entropy model presumption.

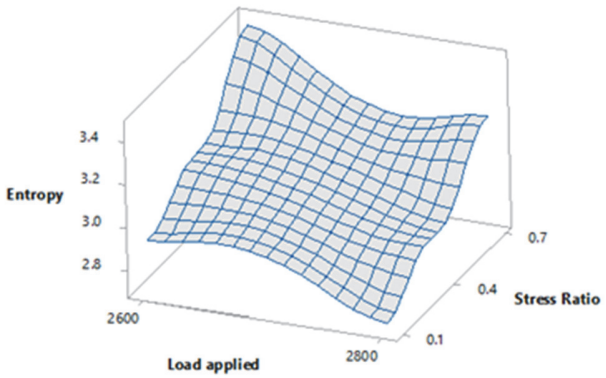

Figure 11: The response surface for entropy MLR-based entropy model

Next, the assumptions of the MLR model were assessed. The four different conditions that need to be evaluated for the multiple regression to give a valid result are the linear function, independent function, normal distribution and equal variance [34]. The results are shown in Fig. 12. Hence, all the MLR-based entropy models justified the requirement that most of the error terms are generally dispersed. When the goodness of fit, homoscedasticity, normality, and linearity of the MLR-based entropy model had been examined, the model was verified by contrasting the entropy values by the models with those observed from the experiment for 3000N, as presented in Fig. 13. From that figure, the entropy anticipated by the MLR-

based entropy model shows noble conformity with the entropy values from the experiments, with an R^2 value of 0.9760. The R^2 value is more significant than 0.9000, which offers the dependability of the model in predicting the entropy of the specimen [33].

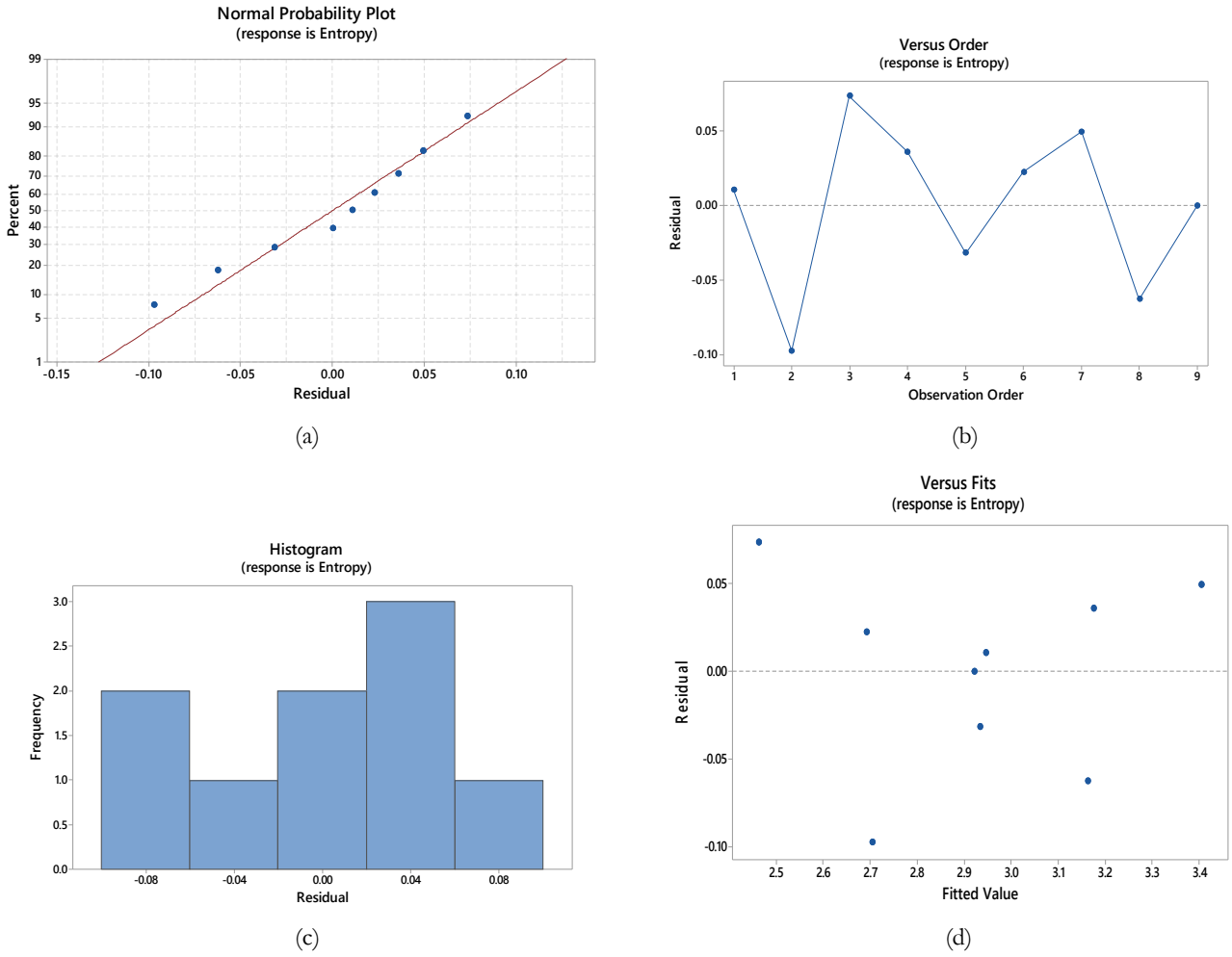

Figure 12: Observation of multiple regression.

Next, the MLR analysis was applied to produce a meaningful entropy prediction model. The set of data that contains the entropy generation values of the CT specimens, stress ratio (R), and load applied (P), as shown in Eqn. (12), was utilised to develop the MLR-based entropy models. The MLR-based entropy generation model or also known as the predicted entropy (γ) was obtained as:

$$\gamma = 5.827 - 0.001148P + 0.8044R \tag{15}$$

Therefore, the regression model parameters are:

$\alpha = 5.827$

$\beta_1 = -0.001148$

$\beta_2 = 0.8044$

Once the assumption of the MLR-based entropy model was clarified to be acceptable, the models were compared to the experimental values done with a load of 3,000N. Tab. 4 shows the percentage of the difference between the experimental and predicted data for 3,000N load conditions. The difference is less than 10%, and the determined entropy generation well

forecasts the experimental data under new load conditions. This shows that the majority of the predicted entropy generation was near to a comparable experimental value.

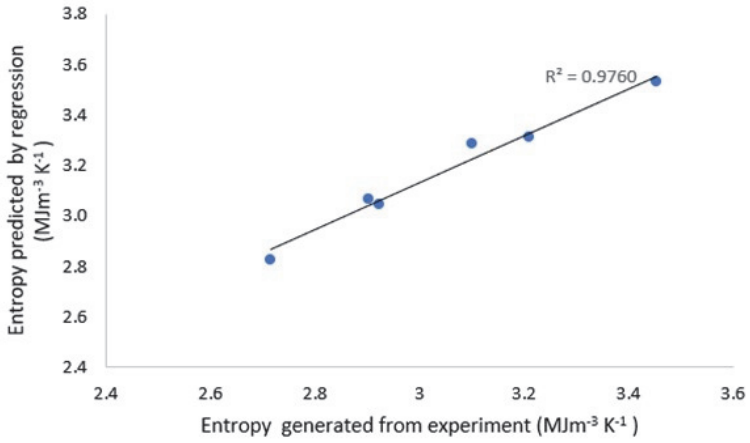

Figure 13: Comparison between the entropy predicted by the MLR-based entropy and entropy observed from the experiment for load 3000N.

Stress ratio	Experimental entropy	Predicted entropy	% of differences
0.1	2.956	3.090	4.6%
0.4	2.607	2.849	9.3%
0.7	2.536	2.608	2.8%

Table 3: The percentage of difference entropy generation concerning the experimental data for 3000N.

CONCLUSIONS

This research shows that entropy generation was deployed as an effective way of measuring the crack growth behaviour of a material with changes in temperature during the fatigue process. The tests were done using compact tension made of AZ31B magnesium alloy for load ratios of 0.1, 0.4, and 0.7 with different loads of 2,600N, 2,800N and 3,000N. The fatigue crack growth life increased with a decrease in the value of the stress ratio. An approach to developing the MLR relationship between the entropy generation applied load and stress ratio was shown in this paper. The assessment of entropy generation through energy dissipation is needed by using an analytical method. Throughout the fatigue test, the entropy generation can be determined from the temperature evolution. By performing compact tension tests, various stress ratios of 0.1, 0.4 and 0.7 were used on the specimen with applied loads of 2,600N, 2,800N and 3,000N. From the test, the lowest entropy generation was 2.536 MJm^{-3} K^{-1} when a 3,000N load with a stress ratio of 0.7 was used for the specimen. Note that the deviation of entropy generation represents a change in the internal friction between the two loads. Therefore, if the entropy generation can be determined and the relationship graphs can be plotted from the fatigue test, then the prediction of the internal friction can be done. As an outcome, the predicted regression model for load 3,000N based on the applied load and stress ratio was discovered to concur with the outcomes of the experiment, with just 9.3% from the real experiment where the entropy values obtained from the experiment and regression model were in good agreement. The results were indeed encouraging, where the percentage difference between the MLR-based entropy models was less than 10%.

Through this study, the data collected also will be beneficial to new approaches to predict fatigue life and get better results such as Artificial Intelligence. Artificial Intelligence is used to solve complex tasks by linking patterns to real-valued quantities by integrating data science and computational resources. An artificial neural network (ANN) is trained on experimentally determined data that is highly relevant in terms of fatigue. Load stress, hardness and defect size are the three main parameters that are defined as input arguments. The main fields of application are pattern recognition, classification, time series forecasting, and signal processing. Artificial neural networks (ANNs) are computing systems started by biological

neurons such as the human brain. ANNs are able to learn from an experience similar to how humans learn. After total fracture occurs at a certain load level, defect size is evaluated by fracture surface analysis. Therefore, various methods have been developed by researchers because there is always a margin for improvement to make fatigue life prediction more accurate.

ACKNOWLEDGMENTS

The authors graciously acknowledge the financial support provided by Universiti Kebangsaan Malaysia (FRGS/1/2019/TK03/UKM/01/3 and DIP-2019-015) and Universiti Pertahanan Nasional (FRGS/1/2018/TK03/UPNM/03/1).

REFERENCE

[1] Xiong, Y., Yu, Q. and Jiang, Y. (2012). Multiaxial fatigue of extruded AZ31B magnesium alloy, Mater. Sci. Eng. A, 546, pp. 119–128. DOI: 10.1016/j.msea.2012.03.039.

[2] Osara, J. A. and Bryant, M. D. (2019). Thermodynamics of fatigue: Degradation-entropy generation methodology for system and process characterization and failure analysis, Entropy, 21(7), pp. 1-24. DOI: 10.3390/e21070685.

[3] Gu, C., Lian, J., Bao, Y. and Münstermann, S. (2019). Microstructure-based fatigue modelling with residual stresses: Prediction of the microcrack initiation around inclusions, Mater. Sci. Eng. A, 751, pp. 133–141. DOI: 10.1016/j.msea.2019.02.058

[4] Kahirdeh, A., Sauerbrunn, C., Yun, H., and Modarres, M. (2017). A parametric approach to acoustic entropy estimation for assessment of fatigue damage, Int. J. Fatigue, 100, pp. 229–237. DOI: 10.1016/j.ijfatigue.2017.03.019.

[5] Wang, Z., et al. (2021). In-situ synchrotron X-ray tomography investigation of damage mechanism of an extruded magnesium alloy in uniaxial low-cycle fatigue with ratcheting, Acta Mater., 211, pp. 1-13. DOI: 10.1016/j.actamat.2021.116881

[6] Wang, X.G., Ran, H.R., Jiang, C., Fang, Q.H. (2018). An energy dissipation-based fatigue crack growth model, Int. J. Fatigue, 114. DOI: 10.1016/j.ijfatigue.2018.05.018

[7] Fan, J. (2018). High Cycle Fatigue Behavior Evaluation of Q235 Steel Based on Energy Dissipation, Jixie Gongcheng Xuebao/Journal Mech. Eng. DOI: 10.3901/JME.2018.06.001.

[8] Meneghetti, G., Ricotta, M., Atzori, B. (2016). The Heat Energy Dissipated in a Control Volume to Correlate the Fatigue Strength of Bluntly and Severely Notched Stainless Steel Specimens, Procedia Struct. Integr., 2, pp. 2076–2083, DOI: 10.1016/j.prostr.2016.06.260.

[9] Meneghetti, G., Ricotta, M., Pitarresi, G. (2019). Infrared thermography-based evaluation of the elastic-plastic J-integral to correlate fatigue crack growth data of a stainless steel, Int. J. Fatigue, 125, pp. 149–160, DOI: 10.1016/j.ijfatigue.2019.03.034.

[10] Wang, X.G., Crupi, V., Jiang, C., Feng, E.S., Guglielmino, E., Wang, C.S. (2017). Energy-based approach for fatigue life prediction of pure copper, Int. J. Fatigue, 104, pp. 243–250. DOI: 10.1016/j.ijfatigue.2017.07.025.

[11] Klingbeil, N.W. (2003). A total dissipated energy theory of fatigue crack growth in ductile solids, Int. J. Fatigue, 25(2), pp. 117–128. DOI: 10.1016/S0142-1123(02)00073-7.

[12] Guo, Q., Guo, X., Fan, J., Syed, R., Wu, C. (2015). An energy method for rapid evaluation of high-cycle fatigue parameters based on intrinsic dissipation, Int. J. Fatigue. DOI: 10.1016/j.ijfatigue.2015.04.016.

[13] Kahirdeh, A., Khonsari, M.M. (2015). Energy dissipation in the course of the fatigue degradation: Mathematical derivation and experimental quantification, Int. J. Solids Struct., 77. DOI: 10.1016/j.ijsolstr.2015.06.032.

[14] Teng, Z., Wu, H., Boller, C., Starke, P. (2020). Thermography in high cycle fatigue short-term evaluation procedures applied to a medium carbon steel, Fatigue Fract. Eng. Mater. Struct., 43(3), pp. 515–26. DOI: 10.1111/ffe.13136.

[15] Mohammadi, B., Mahmoudi, A. (2018). Developing a new model to predict the fatigue life of cross-ply laminates using coupled CDM-entropy generation approach, Theor. Appl. Fract. Mech., 95, pp. 18–27. DOI: 10.1016/j.tafmec.2018.02.012.

[16] Wang, J., Yao, Y. (2017). An entropy based low-cycle fatigue life prediction model for solder materials, Entropy, 19(10). DOI: 10.3390/e19100503.

[17] Teng, Z., Wu, H., Boller, C., Starke, P. (2020). Thermodynamic entropy as a marker of high-cycle fatigue damage accumulation: Example for normalized SAE 1045 steel, Fatigue Fract. Eng. Mater. Struct., 43(12), pp. 2854–2866,

DOI: 10.1111/ffe.13303.
[18] Wang, J., Jiang, W., Wang, Q. (2019). Experimental and numerical evaluation of fatigue crack growth rate based on critical plastically dissipated energy, Int. J. Fatigue, 118, pp. 87–97. DOI: 10.1016/j.ijfatigue.2018.09.003.
[19] Xiao-qing, L., Hong-xia, Z., Zhi-feng, Y., Wen-xian, W., Ya-guo, Z., Qian-ming, Z. (2013). Fatigue life prediction of AZ31B magnesium alloy and its welding joint through infrared thermography, Theor. Appl. Fract. Mech., pp. 1–7. DOI: 10.1016/j.tafmec.2013.10.001.
[20] Ribeiro, P., Petit, J., Gallimard, L. (2020). Experimental determination of entropy and exergy in low cycle fatigue, Int. J. Fatigue, , pp. 105333. DOI: 10.1016/j.ijfatigue.2019.105333
[21] Nourian-Avval, A., Khonsari, M.M. (2021). Rapid prediction of fatigue life based on thermodynamic entropy generation, Int. J. Fatigue, 145, pp. 106105. DOI: 10.1016/j.ijfatigue.2020.106105
[22] Kong, Y.S., Abdullah, S., Schramm, D., Omar, M.Z., Haris, S.M. (2019). Development of multiple linear regression-based models for fatigue life evaluation of automotive coil springs, Mech. Syst. Signal Process., 118, pp. 675–695. DOI: 10.1016/j.ymssp.2018.09.007.
[23] Hajshirmohammadi, B., Khonsari, M.M. (2020). On the entropy of fatigue crack propagation, Int. J. Fatigue, 133, pp. 105413. DOI: 10.1016/j.ijfatigue.2019.105413.
[24] Rabbolini, S., Beretta, S., Foletti, S. (2016). Fatigue crack growth in low cycle fatigue: An analysis of crack closure based on image correlation, Procedia Struct. Integr., 1, pp. 158–165. DOI: 10.1016/j.prostr.2016.02.022.
[25] Stephens, R.I., Fatemi, A., Stephens, R.R. & Fuchs, H.O. (2000). Metal Fatigue in Engineering, 2nd Edition. United States of America, John Wiley & Sons.
[26] Jang, J.Y., Khonsari, M.M. (2018). On the evaluation of fracture fatigue entropy, Theor. Appl. Fract. Mech., 96, pp. 351–361. DOI: 10.1016/j.tafmec.2018.05.013.
[27] Ontiveros, V., Amiri, M., Kahirdeh, A., Modarres, M. (2017). Thermodynamic entropy generation in the course of the fatigue crack initiation, Fatigue Fract. Eng. Mater. Struct., 40(3). DOI: 10.1111/ffe.12506.
[28] Naderi, M., Amiri, M., Khonsari, M.M. (2010). On the thermodynamic entropy of fatigue fracture, Proc. R. Soc. A Math. Phys. Eng. Sci., 466(2114), pp. 423–438, DOI: 10.1098/rspa.2009.0348.
[29] Liakat, M., Khonsari, M.M. (2014). Rapid estimation of fatigue entropy and toughness in metals, Mater. Des., 62, pp. 149–157. DOI: 10.1098/rspa.2009.0348.
[30] Mansor, N.I.I., Abdullah, S., Ariffin, A.K. (2017). Discrepancies of fatigue crack growth behaviour of API X65 steel, J. Mech. Sci. Technol., 31(10), pp. 4719–4726. DOI: 10.1007/s12206-017-0918-2.
[31] Asadi, S., Amiri, S.S., Mottahedi, M. (2014). On the Development of Multi-Linear Regression Analysis to Assess Energy Consumption in the Early Stages of Building Design, Energy Build. DOI: 10.1016/j.enbuild.2014.07.096.
[32] Gope, P. (1999). Determination of sample size for estimation of fatigue life by using Weibull or log-normal distribution, Int. J. Fatigue, 21(8), pp. 745–752. DOI: 10.1016/S0142-1123(99)00048-1.
[33] Castillo, E., Fernández-Canteli, A., Pinto, H., López-Aenlle, M. (2008). A general regression model for statistical analysis of strain-life fatigue data, Mater. Lett., 62(21–22), pp. 3639–3642. DOI: 10.1016/j.matlet.2008.04.015.
[34] Ciulla, G., Amico, A.D. (2019). Building energy performance forecasting: A multiple linear regression approach, Appl. Energy, 253, pp. 113500. DOI: 10.1016/j.apenergy.2019.113500.